PEN00298

Engineer: Fournier & Penland

TEST LOG

UPWT (Test Sec. 1) TUNNEL — MODEL X-24C-L301

TEST NUMBER _____ M = 1.5, 2.0, 2.36, & 2.86 — MOMENT REFERENCE 0.650 ℓ

DATE Dec. 13 → 24, 1976 (Fixed Transition) — REYNOLDS NUMBER _____

PRIORITY	MODEL CONFIGURATION	SURFACE DEFLECTION δ_{e_L}	δ_{e_R}	$\delta_{V_{UL}}$	$\delta_{V_{UR}}$	δ_F	RUN NUMBERS $\alpha = -5° \rightarrow 20°$ $\beta = 0°$	$\beta = 3°$
7	$B_C W V_L V_U E$ Trim	+10	+10	0	0	0	•	
1		0	0				•	•
3		-10	-10				•	
4		-20	-20				•	
5	Roll Control	-10	+10	0	0	0	•	
6	Yaw Control	0	0	-5°	-5°	0	•	
2	$B_C W V_L V_U$ Trim	0	0	0	0	0	•	•
8	" "	-10	-10	0	0	0	•	
9	$B_C W V_L E$	0	0	0	—	0	•	•
10	$B_C W V_U E$	0	0	—	0	0	•	•
12	$B_C W V_L$	0	0	0	—	0	•	•
13	$B_C W$	0	0	—	—	0	•	•
11	$B_C W V_U$							

Data Reduction: L-301

Call to Doug Taylor 10-27-76

His Gen Prog. does --

1. Rotate Bal. to Body (model) Axes
2. Trans Bal. to Bod. {Model Axes Trans}
3. Base Press corr.

838-4043

- LTPT Model Axes Trans.
- 8'TPT ? " "
- UPWT Model " "
- 20" M=6 ? " "

Import. To Know —

- Defin. of angle of wind off α

Call to Keyes — 10-27-76

20" Tn. Program Sequence

1. Base Pres. Corr.
2. Rotate in Roll Bal. to Model ϕ
3. Transfer Mom. (Bal. Axes. Transfers)
4. Rotate Bal. to Model Axes.

[redacted] Copy

Engineer: Fournier & Pen

TEST LOG

UPWT (Test Sec. 1) TUNNEL

MODEL X-24C-13

TEST NUMBER _____ M = 1.5, 2.0, 2.36, & 2.86

MOMENT REFEREN

DATE Dec. 13 → 24, 1976 (Fixed Transition)

REYNOLDS NUMBE

PRIORITY	MODEL CONFIGURATION	SURFACE DEFLECTION δ_{e_L}	δ_{e_R}	$\delta_{V_{UL}}$	$\delta_{V_{UR}}$	δ_F	RUN NUMBERS $\alpha = -5° \rightarrow 20°$ $\beta = 0°$	$\beta = 3°$	Run $\beta = 0°$
7	BcWVLVUE Trim	+10	+10	0	0	0			25,26,27,28
1	"	0	0	"	"	"			(2)(4)(7)(11)
3	"	-10	-10	"	"	"			13,14,15,16
4	"	-20	-20	"	"	"			21,22,23,24
5	" Roll Control	+10	~~X~~0	0	0	0			17,18,19,20
6	" Yaw Control	0	0	+5°	+5°	0			29,30,31,32 *
11	BcWVu (No Eng. or Low Vert)	0	0	0	0	0			(49)(51)(53)(55)
2	BcWVLVu (No Eng.) Trim	0	0	0	0	0			(57)(59)(61)(63) *
8	" (No Eng) "	-10	-10	0	0	0			65,66,67,68
9	BcWVLE (No Upper Vert)	0	0	→	—	0			33,35,37,39
10	BcWVUE (No Lower Vert.)	0	0	⊙	0	0			41,43,45,47
12	BcVLVL	0	0	→	—	0			69,71,73,75
13	BcW	0	0	—	—	0			77,79,81,83
	"VLE (Invented)	0	0	0	0	0			(1)6,9,10 *

* (N), Indic

78-37

Aerodynamic Heating to the Hypersonic Research Aircraft X-24C

R.D. Neumann, J.L. Patterson and N.J. Sliski, *Flight Dynamics Lab, Wright-Patterson AFB, Ohio*

AIAA 16TH AEROSPACE SCIENCES MEETING

Huntsville, Alabama/January 16-18, 1978

AERODYNAMIC HEATING TO THE HYPERSONIC RESEARCH AIRCRAFT, X-24C

R.D. Neumann, Technical Manager
J.L. Patterson, Aerospace Engineer
N.J. Sliski, Aerospace Engineer
High Speed Aero Performance Branch
Air Force Flight Dynamics Laboratory
Wright-Patterson Air Force Base, Ohio

Abstract

The paper discusses the aerodynamic heating environment sustained by the X-24C aircraft evaluated from ground test data taken at the Arnold Engineering Development Center (AEDC), and from engineering design techniques including computer solutions appropriate for the preliminary design process. The objectives of the study were to present problem areas implicit in the design of a complex, high speed aircraft of this type through analysis of the experimental results, and to indicate techniques of data correlation which will reduce tunnel induced uncertainty. The paper shows that through proper evaluation of the recovery factor, data from all the hypersonic tunnels of the von Karman facility at AEDC can be brought into agreement. The data show that the lower surface is not directly predictable by strip theory and that unexpected flow distortions occur near the centerline; that the fuselage sides and strake regions require careful attention to specification of streamline origin and careful analyses of the data to assure turbulent flow in the experiment; that unpredictable hot streaks emanate from the strake-body juncture at low angles of attack; and that the upper surface is a highly unpredictable region of separated, high-energy, vortical flow.

Nomenclature

H	Heat transfer coefficient
M	Mach number
P	Pressure
$\dot{Q}$	Heat transfer rate
Re	Reynolds number
Re_∞/ft	Free-stream unit Reynolds number
s	Streamline length
S_T	Stanton number
T	Temperature
T*	Eckert reference temperature
Y	Spanwise distance
α	Angle of attack
δ	Control surface deflection angle
ϕ	Angular distance around periphery from bottom centerline

Subscripts

L	Over-all model length
ℓ	Local conditions
o	Stagnation conditions
R	Recovery conditions
s	Reference length in streamline direction
T	Based on stagnation temperature
w	Body surface conditions
x	Reference length parallel to model axis
∞	Freestream conditions

Introduction

Flight operations at Mach 6 and beyond, as in the case of the X-15 aircraft, require an understanding of the aerodynamic heating and its influence on the structure and sub-systems of such an aircraft. The Air Force Flight Dynamics Laboratory has evaluated a candidate successor to the X-15 which has been designated the X-24C. This aircraft is a lifting body design capable of sustained operations at Mach 6. The present paper discusses the aerodynamic heating environment sustained by this aircraft evaluated from ground test data taken at Arnold Engineering Development Center (AEDC), and from engineering design techniques including computer solutions appropriate for the preliminary design process.

The paper is not intended to propose this particular configuration for fabrication and flight nor is it focused solely on demonstrating perfect agreement between theory and data. Test evaluation of this configuration presented the Flight Dynamics Laboratory an opportunity to explore techniques of experimentation and to observe problem areas implicit in the design of this class of complex, high Mach number aircraft. It is these insights into test techniques and problem areas that will be explored in the present paper.

The X-24C Vehicle

The X-24C is one class of high L/D lifting body vehicles being studied as the next generation manned research aircraft. In concept, it is similar to the X-15 aircraft. The X-24C would be an air launched, rocket powered configuration capable of flight operations at, and in excess of, Mach 6 at dynamic pressures of 1000 psf or less. The vehicle would serve as a test bed for experimental programs ranging from cryogenically cooled structures to advanced ramjet/scramjet propulsion systems. The design studied in the heat transfer program being reported herein is designated the X-24C-10D and is one of a series of vehicles evaluated under the X-24C study. The X-24C-10D flight configuration is shown in Figure 1.

The Data Base

Wind Tunnel Data

Test data were taken in the large wind tunnels of the von Karman facility of the Arnold Engineering Development Center. Data were taken in Tunnels "A" and "B," large continuous flow facilities which operate at Mach numbers of 5, 6, and 8, and in Tunnel "F," an impulse facility operated near Mach 7. The continuous facilities were used over a range of Reynolds numbers up to the limit of their capability. Tunnel "F" was operated about the flight Reynolds number limit of the aircraft. Figure 2 indicates the actual test points achieved in relationship to the design flight conditions.

Model Data

To support the design process on the X-24C, a full set of 4.75% scale wind tunnel models were fabricated by the Martin Marietta Corporation under Air Force contract. These models were fabricated of stainless steel to measure forces and moments, surface pressures, and aerodynamic heating inferred through thermocouple data. The model scale was selected to maximize the model size which could be tested both in the AEDC high speed wind tunnels and in the 4'x4' transonic facility. The model scale was verified by blockage tests conducted in both the 4'x4' and 16'x16' transonic tunnels as reported in reference 1.

Both surface pressure data and thermocouple data were taken on a single model frame through the use of replaceable model panels. Conventional thick skin machined surfaces were used for pressure tests and electro-formed nickel panels were employed for heat transfer tests. The complex electro-forming process was conducted by the Orlando Division of the Martin Marietta Corp. While the fabrication of these panels, many of which contained complex curvature and deep draws, was not without difficulty, the final parts were outstanding examples of the contemporary art of electroforming.

Surface pressure data were taken at many of the same locations as the heat transfer data and, in all, 250 pressure taps were read at each test condition. This large number, larger than normally possible at AEDC at one time, was achieved by use of internally mounted scanivalve devices in place of the tunnel pressure transducer system. This technique allowed more data to be obtained; however, the data accuracy was somewhat reduced since only a single transducer was used for a range of pressures normally measured by the standard tunnel system of three transducers. In addition, the scanivalve system, which is normally used at transonic speeds, was now used at Mach 6 requiring the thermal protection of the scanivalves and transducers themselves. The resulting test system achieved the anticipated data but introduced operational problems due to system maintenance and internal model complexity which should be thoughtfully considered before scanivalves are again used at these conditions.

Heat transfer data were taken mainly on the complex aft section of the model, i.e., at model station 20.52 and beyond. The original test plan called for the use of locally thin skin panels in the afterbody and knockout pressure taps in the forebody region where Gardon type gages would be installed. The knock-out taps were not used because it was felt that existing data would adequately predict forebody heating and because the emphasis had changed from generating design data to understanding phenomena. Gardon gages were used quite successfully in special purpose tests elsewhere in the test program.

Thin-skin heat transfer data were generated using approximately 200 thermocouples attached (with considerable difficulty) to the electroformed panels. Data loss due to gage detachment was significant due to the difficulty in welding the iron-constantan thermocouples to the nickel surface. This loss amounted to 15% of the gages installed. The model aft section was heavily instrumented at selected body stations with careful attention being paid to potential interference regions.

Control surface areas required special attention because the geometric cross-sections were too thin for thermocouple attachment and required too great a flexibility for egress of the wires. It was decided to use temperature sensitive paint in these regions, fabricating the surfaces of teflon and backing the teflon with steel sheet for strength. The resulting teflon was about 0.10 inches thick, leading to a requirement to take data within the first 10 seconds after model injection - after injection errors were diminished, but before the thermal model was invalidated.

Oil flow data were also taken on the model to support the interpretation of the paint data. These data were taken using the oil dot technique wherein innumerable discrete "dots" were applied. This technique was particularly useful in observing divergent flow regions where high heating rates occur, and in qualitatively interpreting shear using streak length.

Problems of Data Interpretation

Early in the planning for the experimental program several questions were raised which are of fundamental importance in understanding the data. These revolved about how turbulent flow over the body would be assured and how the data would be reduced for comparative purposes between facilities.

The problem of assuring early transition was evaluated by experimentally measuring heat flux on the model in the presence of trip strips located about the nose and along the leading edges as shown in Figure 3. For this exploratory effort, Gardon type gages were imbedded in the force model and data were taken varying the freestream Reynold number and systematically removing the trip strips. At most gage locations little difference in heating rates was noted, indicating that trip devices were not required.

Data on the vehicle side close to the leading edge were affected by tripping. Figure 4 shows measurements taken both with a nose trip ring only, and with no trip devices, compared to a fully tripped case at the gage location shown. Note that tripping is required to generate fully developed turbulent data at this particular gage location. Such tripping must include both nose and leading edge trip strips to be effective over the entire angle of attack range from 0° to 20°. The nose trip ring alone is totally ineffective for angles of attack greater than 6°. This suggests that streamlines sweeping over the vehicle sides at even moderate angles of attack (α = 10°) originate along the leading edge rather than at the vehicle nose. Since the investigation showed that turbulent flow existed for all gage locations except for those on the side, no trip mechanism was employed for the remainder of the test program. However, since some of the side-body data was shown to be laminar, careful attention was given to the remainder of the side-body data to assure that it was, in fact, turbulent.

The second area of concern was data compatibility among the various tunnels used; specifically, what forcing temperature should be applied to the data in forming the Stanton number? Past use of

arbitrary temperatures, either total temperature or some percentage of total temperature, was not satisfactory. Thus, it was decided to use the unique capabilities of Tunnel "A" to generate recovery temperature data. Transient heat flux data were taken in Tunnel "A" varying both tunnel total temperature, T_o, and injected model wall temperature, T_w, in order to vary the heating rate. A linear least squares curve fit to these data was then determined. The recovery temperature was interpreted as the value of the ratio, T_w/T_o, at zero heat flux. This is shown in Figure 5. A separate recovery temperature was generated for each gage by this technique. These recovery temperatures were then used to determine the more general recovery factors which were applied to all the data. Figure 6 indicates the uncorrected and corrected data generated by this technique. The agreement and need for such corrected data are obvious. All data presented in this paper are so corrected.

Discussion of Pressure and Heating Data

The Model Station 20.52 Data

The data at model station 20.52 were selected for an in-depth investigation because this station is sufficiently far aft of the nose to be under turbulent boundary layer flow, it is representative of the cross-sectional geometry of the X-24C, and it is not influenced by the complexities of strakes, fins and control elements.

Figure 7 presents a correlation of the peripheral heat transfer data at the trim angle of attack of 6 degrees. The correlation was made assuming the flow to be turbulent and the model scale to be constant, thus $S_{t_r} R_{e_\infty}^{0.2}$ ft = constant. The Stanton number, S_{t_r}, is based on the recovery temperature previously described. Agreement between the tunnel data at widely varying test conditions is apparent on the lower and side surfaces of the configuration; however, there is a divergence of data in the recompression region on the body near the top centerline of the model. Specifically, increasing the test Mach number decreases the size of the recompression region although it does not affect the final level of heating on the top centerline.

Now, consider the prediction of heating to the surface at this body station. Primary attention will be placed on the lower surface of the wing, the side surface of the fuselage, and the upper centerline of the configuration. The prediction of heating requires that both the level of pressure and the streamline length be accurately determined in order to evaluate the heating rate from equations which are based on simplified two dimensional techniques.

Determination of Pressure Levels

Two numerical techniques were used to predict the level of pressure on the X-24C vehicle at angle of attack. These were the Hypersonic Arbitrary Body Program (HABP), and the shock capturing technique embodied in the Naval Surface Weapons Center (NSWC) code. The arbitrary body program is essentially a bookkeeping technique in which an arbitrary geometry is segmented into elemental panels each of which is evaluated independently as a flat plate at angle of attack to the freestream velocity vector. The shock capturing technique developed by Jay Solomon at NSWC (see reference 2) is a finite differencing technique which does not accurately locate imbedded shocks but smears out their influence on the calculated pressures. Both programs were used for demonstration runs at Mach 6 and compared with existing wind tunnel pressure data at model station 20.52 (see Figure 8). Both programs gave consistent numerical output as to the pressure levels on the lower surface and sides of the fuselage. In the region of expansion from the vehicle side to the upper surface, the NSWC developed code gave superior results, and agreement on the upper centerline of the configuration was surprisingly good for the NSWC code. However, the fatal flaw in the NSWC shock capturing code and, indeed in all codes which use a steady state solution, is the presence of imbedded shock waves due to the leading edge of the vehicle under analysis. The leading edge presented a stagnation line to the flow and created numerical instabilities in the program which shortly caused the program to fail. The arbitrary body program, on the other hand, being a very simple technique which does not consider the vehicle as a whole, continued to generate reasonable pressure level results over large segments of the vehicle. It was for these reasons that the arbitrary body program was selected to use in the calculation of heating to this configuration.

The failure which was experienced by the NSWC code is not a trivial one but a serious limitation of all existing steady state numerical solutions. The alternative use of time dependent techniques, which will circumvent these difficulties, escalates the use of numerical techniques past the level which is acceptable for the design process and requires that, in their place, greater emphasis be placed on semi-empirical techniques such as the arbitrary body program.

Lower Surface Heating

The lower surface of the X-24C, while deceptively simple in geometry, is extremely complex in flow phenomena. In order to examine the features of this heating, data at model station 20.52 across the lower surface span, and data on the lower surface centerline as a function of body station will be discussed. In all cases these data will be referenced to the simplified Eckert flat plate heating theory which is stated as follows:

$$St\, Re_{\infty_x}^{0.2} = 0.0296 \left(\frac{P_1}{P_\infty}\right)^{0.8} \left(\frac{T_\infty}{T^*}\right)^{0.6} \qquad (1)$$

This equation for aerodynamic heating was selected because it is representative of more sophisticated turbulent flat plate heating methods and because data trends, rather than agreement between data and theory magnitudes, were desired. The absence of detailed forebody data containing transitional information makes a more detailed analysis of heating subject to arbitrary assumptions and, hence, suspect.

Model Station 20.52 Data

The distribution of heating rates across the lower surface span at model station 20.52 is shown in Figure 9 for several vehicle angles of attack. The solid lines are linear curve fits through the data. The solid data point on the centerline is an extrapolation of that curve fit to the centerline. Strip theory analysis, based on the assumption that

the streamlines lie parallel to the centerline, in conjunction with simplified Eckert flat plate theory, was used to estimate heating rates on the lower surface. Results of this analysis are shown as the "Theory" line. A comparison of the data trend with strip theory analysis reveals that the central region of the lower surface is highly disturbed and not in agreement with strip theory. Of particular interest is the centerline heating at this station. It can be seen that the centerline data at $\alpha = 1.6°$ are grossly out of agreement with the extrapolation of off-centerline data. This is not an isolated situation. Low angle of attack centerline data exhibit considerable "inflow" which leads to a cold region along the centerline. Immediately outboard of this cold region, a relatively hot peak is observed. Then, nearer the delta wing leading edge, strip theory provides good agreement with the spanwise data trend. It can be seen that considerable care must be exercised in interpreting lower surface heating data properly in order to arrive at a conservative design.

Centerline Data

Centerline data were taken at several model stations and are shown in Figure 10 for angles of attack of 8.4 and 13 Degrees. The open symbols are data and the solid symbols are off-centerline data extrapolations as previously described. The linear solid line is a least squares fit to the data. The curved solid line represents the simplified Eckert flat plate turbulent heating analysis using the solid test point as a reference heating value. What is clearly demonstrated is that centerline heating data at forward model stations have a magnitude far lower than would be predicted by either off-centerline data extrapolation or theory. Further, this anomalous behavior is reduced by pitching the model to higher angles of attack.

Within the limitations of the present paper, it is not possible to discuss either the data or the implications of the data in any further detail. It is important to note, however, that the normal practice of taking only centerline data as representative of lower surface heating is not valid, and will yield substantial errors in the evaluation of the thermal protection system of such a highly swept configuration. Further, these heating patterns which have been widely observed on highly swept delta wings will give rise to substantial thermal gradients which are not predicted by theory but which must be contended with in the design process.

Side Fuselage Heating

The heating to the sides of the fuselage was calculated using pressure data derived from the Hypersonic Arbitrary Body Program (HABP) and streamline length data derived from geometric considerations of the model. As an example, a representative data point on the side of the fuselage was evaluated. Figure 11 indicates the calculated streamline lengths to the point in question and the calculated pressure data compared with the measured surface pressure data. The heat transfer data were calculated using the simplification of the Eckert equation previously described.

Heat transfer data were compared with this theory for both the cases of the streamline length equal to the model station, and for the case of the streamline length derived from the geometry of the situation. These cases are shown in Figure 12. While neither method indicates perfect agreement of data with theory, the use of the variable streamline length improves the agreement significantly. Further, the lesser slope of the curve with increasing angle of attack of the model indicates improved data agreement and the correctness of using a variable streamline distance with angle of attack. It appears from the data that the actual streamline curvature may be somewhat greater than that predicted by geometry, as should be the case in a boundary layer, however, existing agreement is considered satisfactory.

In order to evaluate the 20 to 30 percent disagreement between the data and the theory using the Newtonian streamline length, all the data on the sides of the fuselage were plotted as a function of the freestream Reynolds number using that streamline length as shown in Figure 13. These data were for three gage stations on the side of the fuselage and for four Reynolds numbers at Mach 6. Implicit in this correction is the assumption that the pressure on the side of the vehicle is constant in this region - as we observe from analysis if not from data. These data indicate that with increasing angle of attack, the streamlines shorten, and the data move from fully turbulent toward the region of overshoot observed in transitional heating data. At the low angles of attack this correlation indicates that the full data trend approaches, quite accurately, the theory. At higher angles of attack there are not data sufficiently far from the region of transitional overshoot to prove that statement, although it is a reasonable extrapolation.

Returning to Figure 12, the line marked "A" was derived from the highest Reynolds number data points observed on the fuselage sides. These points are noted as half-filled symbols in Figure 13. Their application indicates improved agreement between data and theory as the Reynolds number of the flow increases and the boundary layer becomes firmly turbulent.

From the study it is concluded that the agreement between data and theory is excellent when the Newtonian streamline distance is used and when the data are not affected by transitional overshoot phenomena. It is further observed that representative data are difficult to obtain in the environment of Tunnel "B" at AEDC due to the low effective Reynolds numbers on the model.

Upper Surface Heating

The top centerline data is shown in Figure 14. The data shown is for 0° angle of attack because this is the peak heating orientation for the upper surface. It can be seen that tunnel freestream unit Reynolds number of approximately $3(10^6)$ per foot was required to produce fully turbulent flow on the upper surface at Mach 6, and that turbulent flow never was achieved at Mach 8. Note that there is very good agreement between tunnels for the fully turbulent flow data. Also shown are the flat plate heating values calculated using pressures from the NSWC program assuming a streamline origin aft of the canopy. The higher experimental heating values relative to the theoretical are due to thinning of the boundary layer resulting from the outflow present on the wind tunnel model.

Body Strake Region

The body strake is a winglike structure set a

dihedral angle of 30°. Because the flow streamlines originate at the strake leading edge there was concern that the heating on this portion of the model might not be turbulent. This region was evaluated, as in the previous discussions, by calculating the local impact angle of the strake with respect to the freestream, and the streamlines based on the geometry of the flow, and then employing these data together with the Eckert flat plate equation to obtain heat transfer data. As an example, data near the trailing edge of the strake were evaluated. These data points are shown in Figure 15. Both static pressure data and temperature-time data were taken at each of these stations.

From the geometry of the problem, the local impact angle of the strake lower surface was evaluated and employed, together with oblique shock theory, to generate pressure data. Figure 15 indicates data taken on the strake compared with these oblique shock calculations. While some spanwise pressure gradients are apparent on the strake - particularly at the higher angles of attack - agreement between data and theory is reasonably good.

Turning now to the evaluation of heat transfer data; data for the gage nearest the leading edge was evaluated to determine the boundary layer state on the strake. Figure 16 indicates these data plotted against the measured static pressure data for conditions observed in tunnel "B" - at Reynolds numbers per foot of 2×10^6 and 5×10^6. These data indicate clearly that for this location, the heating varies from fully laminar at a Reynolds number of 2×10^6/ft to turbulent at a Reynolds number of 5×10^6/ft. Similar results are observed for all gages at model station 26.84 on the strake (see Figure 17). While some scatter in the data is noted, the correlation indicates that this simplified approach forms an upper limit to the data. As in the case of the fuselage sides, previously discussed, all data on the strake at model station 26.84 and at various unit Reynolds numbers were plotted as a function of the freestream Reynolds number to the gage as shown in Figure 18. These data, while not as cohesive as that on the sides, indicate fully developed turbulent flow for Reynolds numbers of the order of 2×10^6 and agreement between peak turbulent heating and the Eckert formulation. Again, as in the case of the fuselage sides, data were taken in the vicinity of transition and care must be exercised in evaluating the boundary layer state of an arbitrary data point.

Elevon Heating

Based upon the strake heating data, estimates were made of the heating to the strake elevon deflected 20° into the lower surface airflow. The heating increase was calculated by augmenting the strake heating at the hinge line with the pressure rise appropriate to that flap deflection. Figure 19 indicates the pressure rise due to a flap deflection of 20° from data on the X-24C and from theory. The solid line indicates the pressure ratio developed from a geometric evaluation of local flow angles and Mach numbers on the strake. The second line indicates a correction of the theory made by evaluating local flow angles and Mach number from undeflected elevon static pressure data. Both approaches ignore any influence of the body on the strake pressures. It appears reasonable to assume that the difference between data and theory is due to the more complex shock system about the aircraft.

The heating on the deflected elevon is predicted in Figure 20 starting from strake data at model station 26.84. Also shown in this figure are results from thermal paint data for this condition. Reasonable agreement between data and theory is noted considering the basic uncertainty of such paint data. Of particular interest are data taken on the elevon control surface at 4° vehicle angle of attack. Figure 21 indicates one frame of the photographic data taken in the strake region. Both temperature paint data and oil flow data were simultaneously taken and are represented in the figure. The temperature paint data, on the left, indicates a hot streak across the elevon which emanates from the juncture of the strake and fuselage surface. The oilflow data on the right indicates divergent flow over the strake in a streamwise direction which also translates to higher local heating. This phenomenon was only observed at the lower vehicle angles of attack ($\alpha \approx 4°$). Note that paint data were limited to control surfaces so that hot streaks would not appear on the strake itself. Figure 22 indicates the width of the hot streak and iso - heating lines derived from an evaluation of temperature sensitive paint data.

Upper Flap Region

The upper surface region on the X-24C is dominated by vorticity. This can be clearly seen in the oilflow patterns on the upper surface of the model. Such vorticity is a characteristic of lifting reentry vehicles and has been observed on many of the designs.

The upper flaps of the X-24C are placed in this environment. Heating and oilflow data on these flaps demonstrate the vorticity of the flow and that the flow on the leeside is, indeed, highly energetic. Figures 23 through 25 indicate data on the model with these flaps deflected upward 40 degrees into the leeside flow field of the aircraft.

Several features of the flow are defined in Figure 23 with the model at zero angle of attack. The oilflow shows a large vortex motion toward the aircraft centerline impinging on the flap. The heating data indicate that the outer portions of the vortex generate higher heating than the core region. Figure 24 indicates similar data for the model at 4 degrees angle of attack. In this case the increased angle of attack has caused the vortex to move closer to the model centerline and a divergent region has been created on the outer portion of the flap. It is characteristic of such divergent oilflow regions that they are also regions of higher local heating due to a thinning of the boundary layer. This is apparent in the temperature paint data.

At 8 degrees angle of attack the divergent line is also seen (see Figure 25) but it has translated inward toward the centerline of the vehicle and far less vortical movement is observed in the oilflow. Similar features are also observed at model angles of attack of 16 degrees and 20 degrees angle of attack. At these higher angles of attack the vortex system moves off the surface of the body and the divergent line occurs on the outermost portion of the flap. A composite of the heating data on the model configuration as derived from the temperature paint and oil flow data data is shown in Figure 26.

Conclusions

An experimental and analytical study of the X-24C lifting body heating has been presented. It was the goal of this paper not so much to indicate outstanding agreement between data and theory but to present problem areas uncovered in the analysis of the experimental results and to indicate techniques of data correlation which will reduce tunnel induced uncertainty. The following conclusions are thus stressed:

1. That through proper evaluation of the recovery factor, data from all of the hypersonic tunnels of the von Karman facility at AEDC can be brought into agreement. In this respect, it is important to note that Tunnel F, long maligned for data quality, produced data of outstanding quality with data scatter comparable to that of the continuous flow tunnels, "A" and "B."

2. That the lower surface of this highly swept delta wing is not directly predictable by strip theory and produces flow distortions in the location of measurement devices and the analysis of test results.

3. That the sides of the fuselage and strake regions require careful attention to the specification of the streamline length and a careful evaluation of the results in order to assure that they are representative of fully developed turbulent flow.

4. That the strake region at low angle of attack creates a localized hot streak emanating from the juncture of the strake and the body which cannot, at present, be analyzed.

5. That the upper surface separated region is a region of high vortical energy which can impinge on surfaces placed into it.

References

1. J.M. Whoric, "Comparative Analyses of Results from Wind Tunnel Wall Interference Tests in the AEDC Aerodynamic Wind Tunnel (4T) with a 1.3 - Percent Blockage Model," AEDC-TR-75-110, August 1975.

2. J.M. Solomon, et al, "A Program for Computing Steady Inviscid Three-Dimensional Supersonic Flow on Reentry Vehicles," NSWC/WOL/TR 77-28, February 1977.

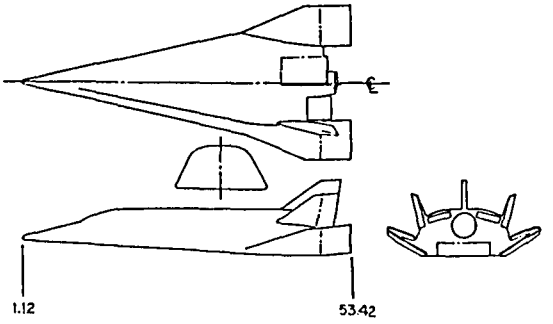

Figure 1 X-24C Flight Configuration

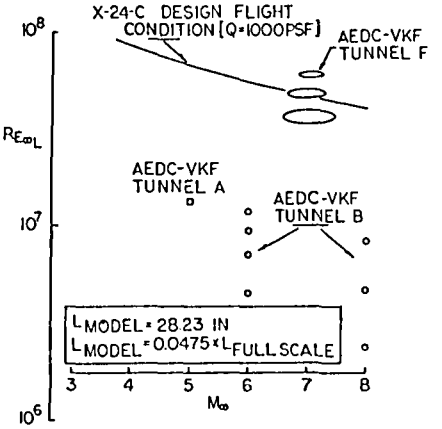

Figure 2 Test Points vs. Limit Flight Conditions

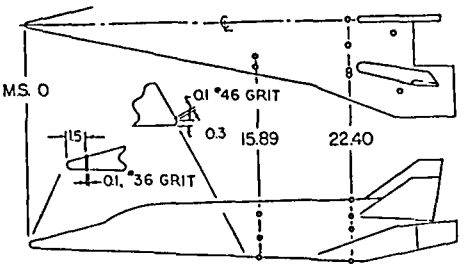

Figure 3 Trip Strip Locations

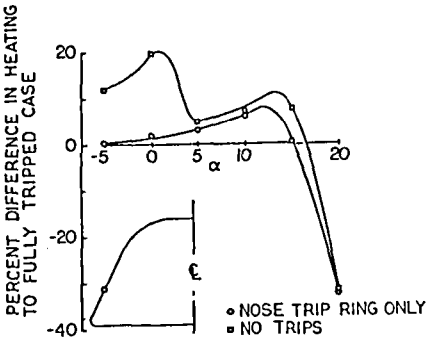

Figure 4 Trip Effects on Side Body Data

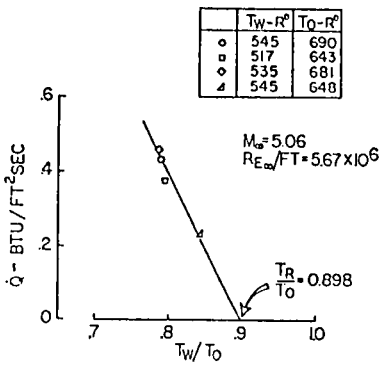

Figure 5 Technique for Determining Recovery Temperature

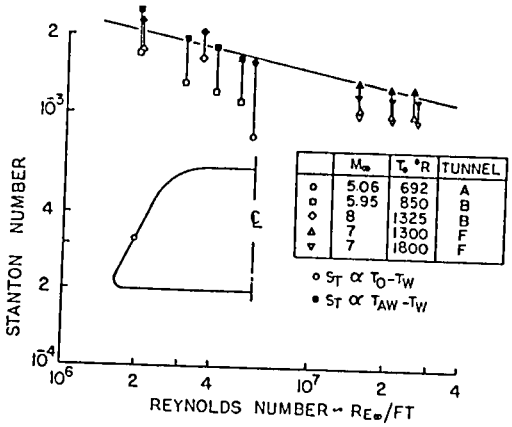

Figure 6 Data Corrected to Recovery Temperature

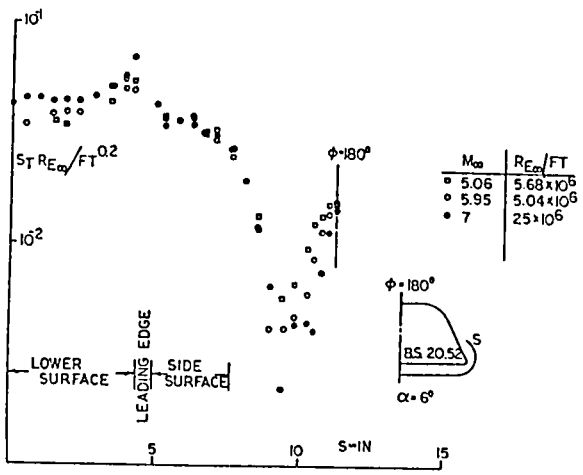

Figure 7 Correlation of Peripheral Heat Transfer Data

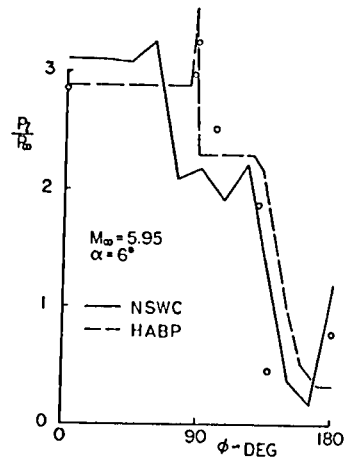

Figure 8 Peripheral Pressure Data Compared to Theoretical Predictions

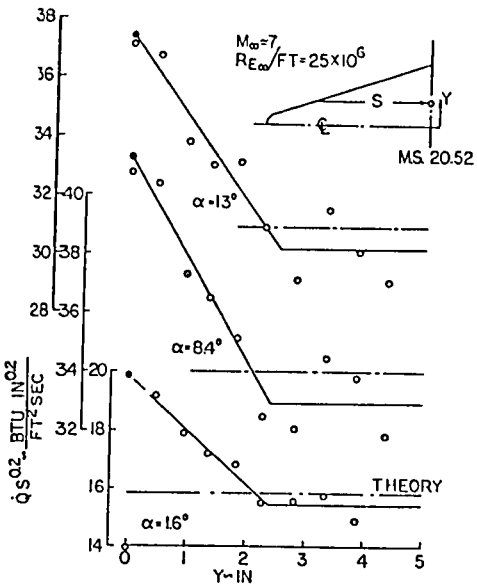

Figure 9 Span-Wise Lower Surface Heating

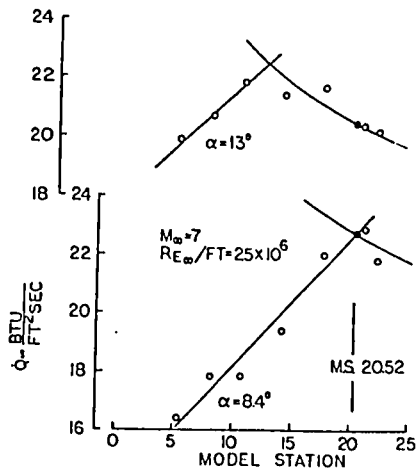

Figure 10 Lower Surface Centerline Heating

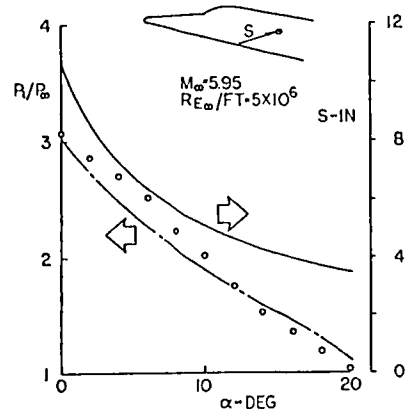

Figure 11 Typical Side Body Streamline Lengths and Pressures

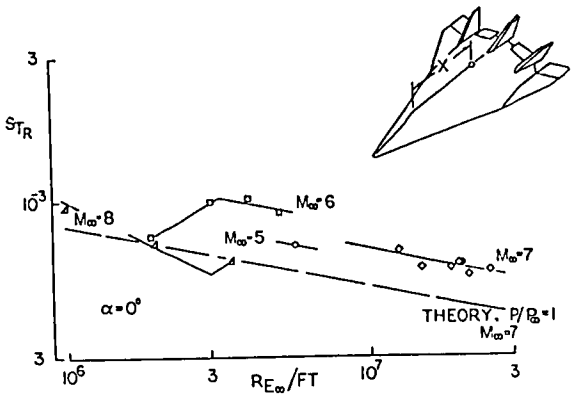

Figure 14 Upper Surface Centerline Heating

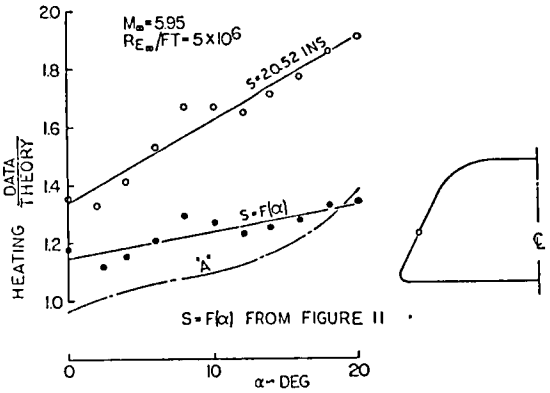

Figure 12 Effect of Streamline Origin on Side Body Heating

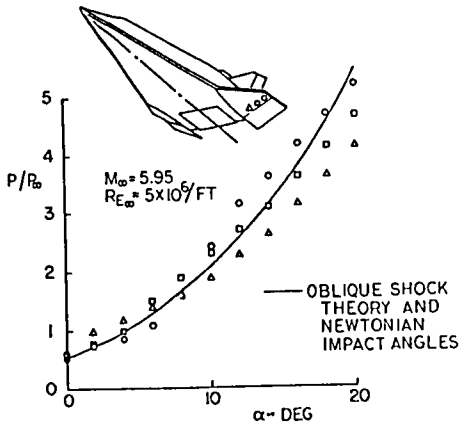

Figure 15 Strake Pressures Compared to Oblique Shock Theory

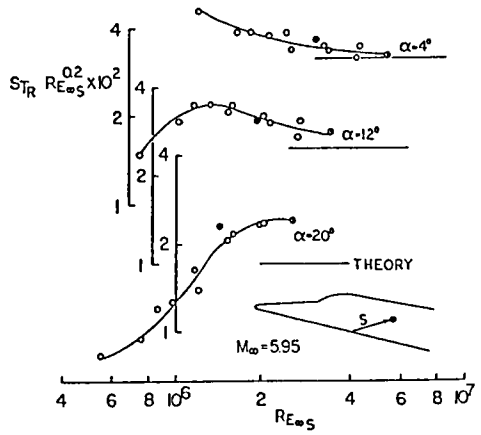

Figure 13 Transition of Heating on Side Surface with Increasing Angle of Attack

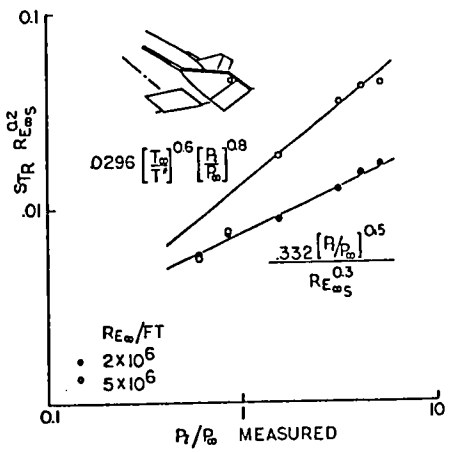

Figure 16 Boundary Layer State on Strake from Gage Nearest Leading Edge

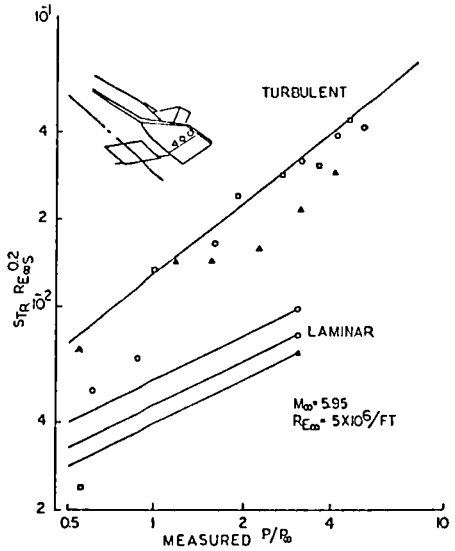

Figure 17 Correlation of Heating Data on Lower Strake Surface

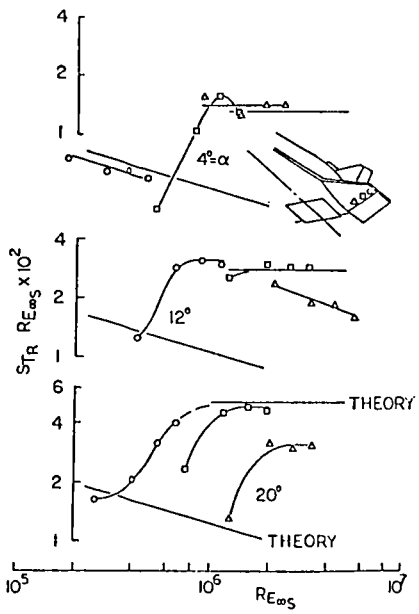

Figure 18 Boundary Layer Transition on Strake as Function of Reynolds Number

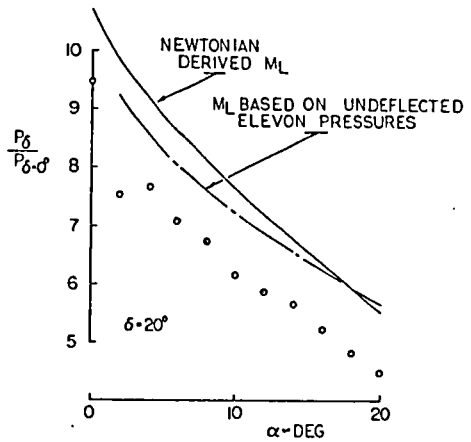

Figure 19 Pressure Rise Due to Elevon Deflection

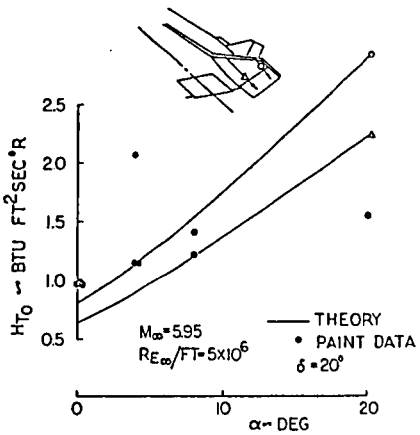

Figure 20 Heating on Deflected Elevon

Figure 21 Temperature Paint and Oil Flow Data for Elevon Lower Surface

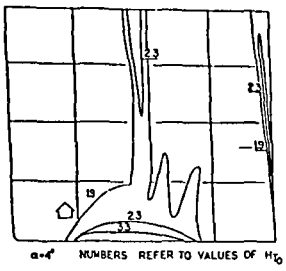

Figure 22 Distribution of Heating on Elevon

Figure 25 Temperature Paint and Oil Flow Data for Upper Surface Flap
$\alpha = 8°$, $\delta = 40°$

Figure 23 Temperature Paint and Oil Flow Data for Upper Surface Flap
$\alpha = 0°$, $\delta = 40°$

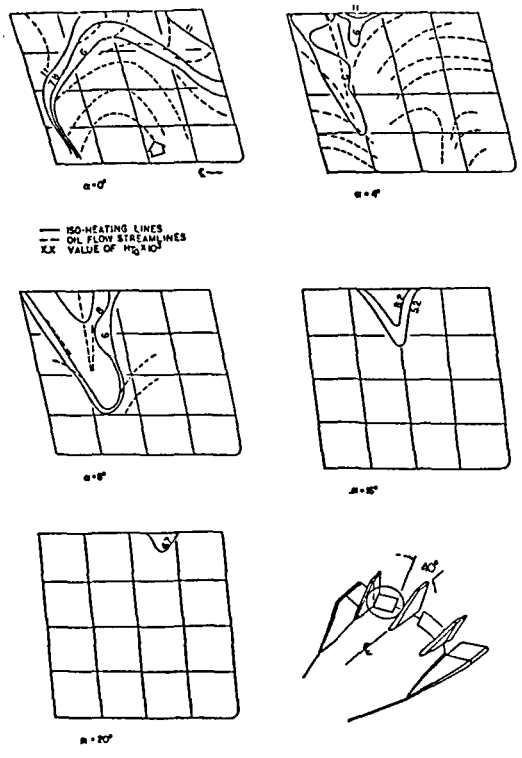

Figure 26 Composite of Heating Data on Deflected Upper Surface Flap

Figure 24 Temperature Paint and Oil Flow Data for Upper Surface Flap
$\alpha = 4°$, $\delta = 40°$